Substitutional Doping of TMDs for Gas sensing Applications

Dissertation submitted to

Visvesvaraya National Institute of Technology, Nagpur

in partial fulfilment of the requirements for the award of the degree

Master of Science
in
Physics

by

Nitesh Prajapati (MS23PHY015)

Under the guidance of

Dr. Poorva Singh

Department of Physics
Visvesvaraya National Institute of Technology
Nagpur 440010 (India)
2024-2025

VISVESVARAYA NATIONAL INSTITUTE OF TECHNOLOGY,
NAGPUR
DEPARTMENT OF PHYSICS

Dissertation approval sheet

Dissertation entitled "**Substitutional Doping of TMDs for Gas sensing Applications**" by **Nitesh Prajapati** Enrollment No. **MS23PHY015** ID No. **30613** is approved for the degree of Master of Science in Physics.

_____

(Name:)

Supervisor

_____

(Name:)

External Examiner

_____

(Name:)

Chairman

Department of Physics

Visvesvaraya National Institute of Technology, Nagpur

Declaration

I, Nitesh Prajapati, hereby declare that this dissertation titled " **Substitutional Doping of TMDs for Gas sensing Applications**" is carried out by me in the Department of Physics of Visvesvaraya National Institute of Technology, Nagpur. The work is original and has not been submitted earlier whole or in part for the award of any degree/diploma at this or any other Institution / University.

Nitesh Prajapati

Date: - -2025

Certificate

This to certify that the dissertation titled "**Substitutional Doping of TMDs for Gas sensing Applications** is submitted by **Nitesh Prajapati** in partial fulfillment of the requirements for the award of the degree of **Master of Science in Physics**, VNIT Nagpur. The work is comprehensive, complete and fit for final evaluation.

Dr. Poorva Singh

Assistant Professor

Physics Dept, VNIT, Nagpur

Head, Department of Physics

VNIT, Nagpur

Date: - -2025

VISVESVARAYA NATIONAL INSTITUTE OF TECHNOLOGY NAGPUR

Non-Plagiarism Certificate

Certified that M.Sc. dissertation titled **"Substitutional Doping of TMDs for Gas sensing Applications"** by **Nitesh Prajapati**, Enrollment No. **MS23PHY015**, ID No. **30613** has been checked for plagiarism using TURNITIN software and overlap is found within prescribed limits. A summary of the report given below;

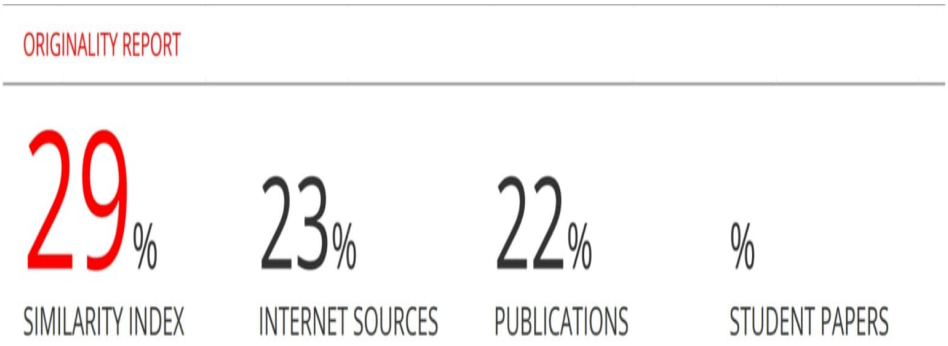

Nitesh Prajapati
MS23PHY015

Dr. Poorva Singh
Supervisor

ACKNOWLEDGEMENT

I would like to convey my gratitude to my project guide Dr. **Poorva Singh** , Assistant Professor, Department of Physics, Visvesvaraya National Institute of Technology Nagpur, for motivating me and guiding me much in my project work. I will be failing in my duty if I do not acknowledge her with a special thanks. This acknowledgement can not represent the the volcano of feelings that is rumbling to burst out of me through words. I feel highly obliged to have her as my guide. I am highly grateful to her for always been the support system. It's been an honour to work with her.

I am highly thankful to Head of the Department,Department of Physics, VNIT Nagpur, **Dr. B. R. Sankpal** and all professors for their precious cooperation throughout the session.

I convey my deep gratitude to **Mr. Nagarjun**, **Mr. Ajit Singh Jhala**, Ph.D. scholars, who had to bear a heavy load of responsibility and concern in bringing this project to a successful end. He has been a great mentor and without him this project would have been a distant reality.

Nitesh Prajapati
MS22PHY015

ABSTRACT

This thesis undertakes a computational exploration of the electronic band structures of mono layered 2D materials when the material is substitutionaly doped . In this, VASP-based DFT calculations are used for the calculation of electronic band structures. In one case adsorption energy and charge transfer is calculated to verify the sensitivity of substitutionally doped TMD.

List of Figures

1.1 Substitutionally Doped TMD 5
1.2 NH_3 Adsorbed TMD 8

2.1 Flow chart for the scf calculation to solve Kohn-Sham equations. . . . 19

3.1 Band structure of mono layered MoS_2 38
3.2 Band structure of Au doped mono layered MoS_2 39
3.3 Band Structure of NH_3 adsorbed Au doped WSe_2 40
3.4 Electron density difference of NH_3 adsorbed on Au-doped WSe_2TMD monolayer 41

NOMENCLATURE

DFT	Density Functional Theory
LDA	Local Density Approximation
GGA	Generalised Gradient Approximation
TBG	Twisted Bilayer Graphene
SPP	Surface Plasmon Polaritons
vdW	Van der Waals
TMD	Transition Metal Dichalcogenides
t-BLG	Twisted Bilayer Graphene
SOC	Spin-Orbit Coupling
QE	Quantum ESPRESSO
CG	Conjugate Gradient
DZP	Double Zeta Polarization
VASP	Vienna Ab-initio Simulation Package
LAMMPS	Large-scale Atomic/Molecular Massively Parallel Simulator
SIESTA	Spanish Initiative for Electronic Simulations with Thousands of Atoms

Table 1

CONTENTS

Abstract **i**

List of Figures **ii**

Nomenclature **iii**

Contents **iv**

1 INTRODUCTION **2**

1.1 Introduction 2

1.2 Transition Metal Dichalcogenides (TMDs) 3

1.3 Mono Layer TMDs 4

1.4 How Mono Layer TMDs are different from Bulk TMDs 5

1.5 Gas sensing mechanism in mono layered TMDs: 6

1.6 Adsorption energy 7

1.6.1 Formula for Adsorption energy 7

1.6.2 Bader Charge Analysis 8

2 CONCEPTS AND COMPUTATIONAL METHODOLOGY **10**

2.1 Approximation Method 10

2.2 The Born-Oppenheimer approximation 11

2.3 Density Functional Theory Approach 12

2.3.1 The Theorems of Hohenberg and Kohn 13

2.3.2 The Kohn-Sham equation 16
2.3.3 The exchange-correlation functional 20
2.3.4 Spin-Orbit Interaction 21
2.4 Solving the equations 22
2.5 Applications of DFT 23
2.5.1 Equilibrium Structure 23
2.5.2 Band Structures and Density of States (DOS) 24
2.6 Computational Package 25
2.6.1 VASP 25
2.6.2 LAMMPS 27
2.6.3 SIESTA 27

3 Results and discussions **31**
3.1 Structural relaxation using VASP 31
3.1.1 POSCAR FILE FOR MoS_2 31
3.1.2 POSCAR FILE FOR WSe_2 32
3.1.3 POSCAR FILE FOR Au DOPED MoS_2 32
3.1.4 POSCAR FILE FOR NH_3 ADSORBED Au DOPED MoS_2 . 35
3.1.5 RELAXED POSCAR (CONTCAR) FILE FOR NH_3 ADSORBED Au-DOPED MoS_2 36
3.2 Electronic band structures 37
3.3 Adsorption energy and charge transfer 40

4 SUMMARY AND CONCLUSION **43**
4.0.1 Summary 43
4.0.2 Conclusion 43

Reference **44**

INTRODUCTION

Chapter 1

INTRODUCTION

1.1 Introduction

Doping is a fundamental technique used to modify various properties of a material, such as electrical conductivity, magnetic behavior, and optical characteristics. It plays a critical role in bandgap engineering and has achieved tremendous success over the past several decades.

Layered two-dimensional (2D) materials—such as graphene and its inorganic analogues like hexagonal boron nitride (hBN), molybdenum disulfide MoS_2, tungsten disulfide WS_2, and other transition metal dichalcogenides (TMDs)—have attracted increasing interest as sensing layers in resistive gas sensors. This is primarily due to the presence of inherent defect sites (particularly at the flake edges) and their large surface-to-volume ratio.

Doping of such 2D materials is crucial (to realize p- and n-type materials) for improving selectivity and enhancing sensing responses toward specific target analytes. In conventional semiconductors like silicon, doping—widely used in microelectronic devices within integrated circuits—is typically achieved through diffusion or ion implantation techniques.

Substitutional doping involves replacing host atoms in a 2D lattice with heteroatoms—for example, boron (B), nitrogen (N), or phosphorus (P) in graphene, and sulfur (S) vacancies in MoS_2 . This technique:

- Tailors electronic properties, such as the bandgap and carrier concentration,
- Introduces active sites for catalysis and gas adsorption,
- Enhances structural stability compared to surface adsorption doping.

This thesis aims to discuss how the band structures are altered when a transition metal dichalcogenide is substitutionally doped, and how the adsorption energies and charge transfers vary across different types of TMDs.

1.2 Transition Metal Dichalcogenides (TMDs)

Transition metal dichalcogenides (TMDs) are a class of two-dimensional (2D) materials with the general formula MX_2, where M represents a transition metal (such as Mo, W, or Re), and X denotes a chalcogen (such as S, Se, or Te). These materials have garnered significant attention due to their unique electrical, optical, mechanical, and chemical properties, making them highly promising for a variety of applications.

TMDs exhibit a layered structure, with each layer consisting of a plane of transition metal atoms sandwiched between two planes of chalcogen atoms. These layers are held together by weak van der Waals forces, which enable easy exfoliation into monolayers.

Notably, the electronic properties of TMDs vary with the number of layers. For instance, bulk MoS_2 has an indirect bandgap of approximately 1.2 eV, whereas monolayer MoS_2 exhibits a direct bandgap of about 1.8 eV. This shift enhances photoluminescence, making monolayer TMDs suitable for optoelectronic applications.

Applications of Transition Metal Dichalcogenides (TMDs)

Electronics and Optoelectronics:

Due to their semiconducting nature and sizable bandgaps, TMDs are widely explored for use in field-effect transistors (FETs), photodetectors, and light-emitting devices. For example, monolayer -based FETs have demonstrated high on/off current ratios and significant photoresponsivity.

Sensing: The large surface-to-volume ratio and the presence of active edge sites in TMDs make them excellent candidates for gas sensing applications. Few-layer MoS_2 nanosheets have shown high sensitivity for detecting gases such as NO.

Energy Storage and Conversion: TMDs are being actively investigated for use in batteries and supercapacitors due to their ability to intercalate ions and support rapid redox reactions. Additionally, their catalytic properties make them suitable for applications such as hydrogen evolution reactions (HER).

Biomedical Applications: Recent studies have explored TMDs for drug delivery, biosensing, and biomedical imaging, leveraging their biocompatibility and distinctive optical properties.

1.3 Mono Layer TMDs

"Monolayer TMDs" refers to monolayer transition metal dichalcogenides, a class of two-dimensional (2D) materials with the general formula MX_2, where:

M = transition metal (e.g., Mo, W)

X = chalcogen (e.g., S, Se, Te)

In their monolayer form, TMDs consist of a single layer of atoms: one layer of

transition metal atoms sandwiched between two layers of chalcogen atoms (X–M–X structure). These materials have attracted considerable interest due to their unique electronic, optical, and mechanical properties that differ significantly from their bulk counterparts.

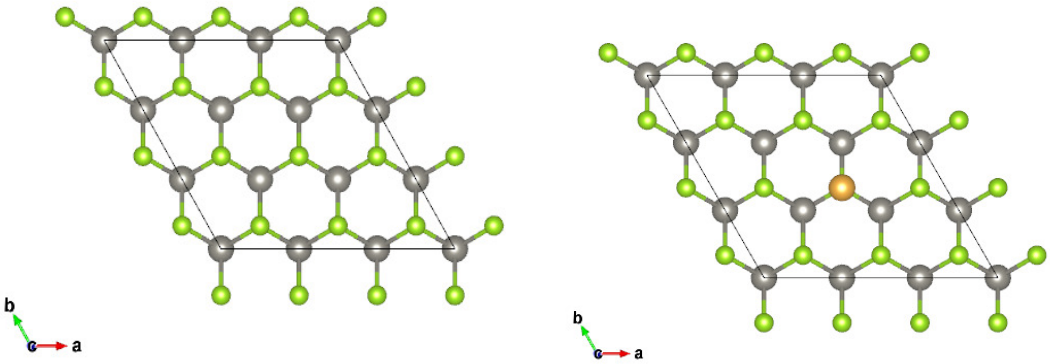

(a) Mono Layered TMD (b) Mono Layered TMD

Figure 1.1: Substitutionally Doped TMD

1.4 How Mono Layer TMDs are different from Bulk TMDs

Monolayer transition metal dichalcogenides (TMDs) displays distinct properties compared to their bulk counterparts, as there is monolayer so no interaction between the layers and due to quantum confinement .Below the detailed comparison is given,

Electronic Properties: Bulk TMDs exhibit indirect band gap whereas monolayered TMDs exhibit direct band gap which is relatively larger. For instance bulk MoS_2 has an indirect band gap of 1.15 eV while monolayered MoS_2 has a direct band gap of approximately 1.90 eV[1].

Optical Properties: As the mono layered TMDs have direct band gap nature so

they show stronger photoluminiscence compared to the bulk. A mono layer of TMD can absorb up to 20 percent of incident light, which is unprecedented for such a thin material[2]

Carrier Mobility: Carrier mobility is often lower in single layered TMDs, influenced by substrate interactions and increased scattering while in bulk generally they exhibit higher carrier mobility due to reduced surface scattering and fewer defects[3].

Dielectric Properties: The dielectric constant of monolayer MoS_2 is remarkably lower than that of bulk, influencing exciton binding energies[4]

Vibrational Properties: Monolayered transition metal dichalcogenides (TMDs) display unique vibrational properties that vary significantly from their bulk counterparts. These differences are primarily due to the decreased dimensionality and the absence of interlayer interactions in monolayer structures[3].

1.5 Gas sensing mechanism in mono layered TMDs:

Monolayer TMDs are magnificent candidates for gas sensing applications, especially for detecting low concentrations of toxic gases like NO_2, NH_3, and H_2S at room temperature, with potential for wearable and portable devices.Gas sensing mechanism in single layered 2D materials are operated through the mechanism mainly like charge transfer, surface adsorption. Due to these mechanism electrical properties of the materials get changed upon exposure to various gas molecules[3]

Charge Transfer Mechanism: Gas sensing mechanism is usually based on charge transfer between the molecules of gas and the sensing material. for example a reducing gas like NH_3 adsorbed onto MoS_2 surface it donates electrons to MoS_2 and increase its electrical conductivity. conversely an oxidizing gas accept electron from the surface reducing electron concentration in the conduction band as a result electrical conductivity is decreased[5].

Surface Adsorption Mechanism: when oxygen atoms in atmosphere adsorb on the surface of sensing material they accept electrons from the surface and create oxygen ions. when any target gas like NH3 adsorbs then these oxygen ions interact with them this leads to increase the conductance[6].

1.6 Adsorption energy

Adsorption energy is defined as the energy released (or required) when a gas molecule binds to the surface of a material. calculating this energy we get the idea that how strongly the gas molecule is interacting with the surface.

. Negative value of adsorption energy indicates that the process os exothermic and it is the thermodynamically possible. More higher negative value of adsorption energy indicates the stronger binding between the gas molecule and the surface atoms or molecules[7]

.If the value of adsorption energy is positive, it shows that the process is endothermic and it is not thermodynamically possible.

1.6.1 Formula for Adsorption energy

We can calculate the adsorption energy by using the formula as:

$$E_{\text{ads}} = E_{\text{gas+surface}} - (E_{\text{surface}} + E_{\text{gas}}) \tag{1.1}$$

- $E_{\text{gas+surface}}$: Total energy of system after gas adsorption.
- E_{surface}: Energy of the surface.
- E_{gas}: energy of the isolated gas molecule.

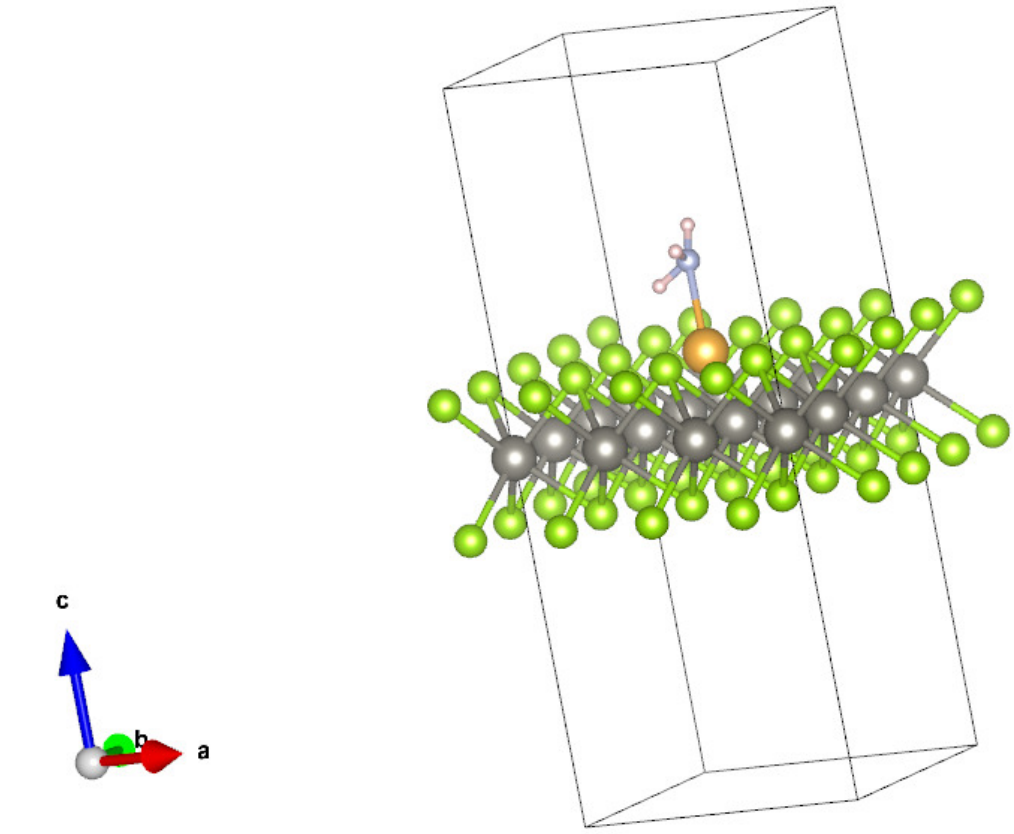

Figure 1.2: NH_3 Adsorbed TMD

1.6.2 Bader Charge Analysis

Bader charge analysis is a method used in computational chemistry and materials science to evaluate the charge distribution within a system. The Bader charge is the total electron density within the volume of the atom. Comparing this to the number of valence electrons of a neutral atom gives an estimate of charge transfer[3].

CONCEPTS AND COMPUTATIONAL METHODOLOGY

Chapter 2

CONCEPTS AND COMPUTATIONAL METHODOLOGY

2.1 Approximation Method

In the realm of quantum mechanics, our aim is to derive a wavefunction that encapsulates all pertinent details regarding the quantum system under investigation. This system could range from a simple free particle, a particle confined in a box, a slightly intricate harmonic oscillator, to more complex entities like the hydrogen atom, helium atom, hydrogen ion, and even more elaborate structures such as molecules, quantum dots, nanotubes, quasi-two dimensional sheets, or crystals. Extracting information from this wavefunction entails solving Schrödinger's equation, which represents the full Hamiltonian of the system, encompassing all interactions within the quantum domain[3].

Considering a solid, we envision it as comprising N heavy, positively charged nuclei and ZN lighter, negatively charged electrons. This configuration presents us with a quantum many-body problem with N+ZN interacting particles, and the corresponding many-particle Hamiltonian is articulated as follows:

$$\hat{H} = \frac{-\hbar^2}{2}\sum_i \frac{\nabla^2_{\vec{R}_i}}{M_i} - \frac{\hbar^2}{2}\sum_i \frac{\nabla^2_{\vec{r}_i}}{m_e} - \frac{1}{4\pi\epsilon_0}\sum_{i,j}\frac{e^2 Z_i}{|\vec{R}_i - \vec{r_j}|} + \frac{1}{8\pi\epsilon_0}\sum_{i\neq j}\frac{e^2}{|\vec{r_i} - \vec{r_j}|} + \frac{1}{8\pi\epsilon_0}\sum_{i\neq j}\frac{e^2 Z_i Z_j}{|\vec{R}_i - \vec{R}_j|} \tag{2.1}$$

The mass of the nucleus at $\vec{R}_i$ is M_i , the electrons have mass m_e and are at $\vec{r_i}$ .The first two terms in the Hamiltonian correspond to the kinetic energy operators for nuclei and electrons, respectively. The subsequent terms delineate the Coulombic interactions among electrons and nuclei, electrons among themselves, and nuclei with each other. However, solving this comprehensive Hamiltonian exactly is infeasible. Nonetheless, through a series of approximations, we can derive acceptable approximate eigenstates, facilitating the extraction of various insights about the system[3].

2.2 The Born-Oppenheimer approximation

In this approximation, we opt to immobilize the N nuclei at their respective positions due to their significantly greater mass and reduced mobility compared to electrons. Consequently, our many-body problem now revolves solely around the behavior of electrons. The fixed nuclei serve as the 'external' entities relative to the electron cloud[8].

Upon implementing this approximation, the many-body problem transforms into a many-electron system. Herein, we contend with a cohort of NZ interacting electrons, navigating within the given potential field created by the immobilized nuclei.

After fixing the ionic coordinates R_i in space, the simplified Hamiltonian for electrons, adhering to the Born-Oppenheimer approximation, is delineated as:

$$\hat{H} = -\hbar^2/2\sum_i \frac{\nabla^2_{\vec{r}_i}}{m_e} - \frac{1}{4\pi\epsilon_0}\sum_{i,j}\frac{e^2 Z_i}{|\vec{R}_i - \vec{r_j}|} + \frac{1}{8\pi\epsilon_0}\sum_{i\neq j}\frac{e^2}{|\vec{r_i} - \vec{r_j}|} \tag{2.2}$$

It's crucial to note that in this formulation, we haven't accounted for electron-phonon scattering or temperature effects, as our focus remains on describing the Hamiltonian

for a solid. Formally, we express this as:

$$\hat{H} = \hat{T} + \hat{V_{ext}} + \hat{V} \tag{2.3}$$

Here, the Hamiltonian encompasses solely the kinetic energy of the electron gas ($\hat{T}$), the potential energy attributed to electron-electron interactions ($\hat{V}$) and the potential energy of electrons in the now external potential field of the immobilized nuclei ($\hat{V_{ext}}$).

2.3 Density Functional Theory Approach

After applying the Born-Oppenheimer approximation, the resultant quantum many-body problem, represented by equation (2.2), is notably simpler compared to its original form, equation (2.1). Nonetheless, solving it exactly remains exceedingly challenging. To tackle this complexity, various methods aim to further simplify equation (2.2) into a more manageable and approximate format. Among these, the *Thomas-Fermi model* and the *Hartree-Fock model*,hold paramount importance and are extensively discussed in condensed matter physics [9].

The *T-F model* marks the pioneering attempt to utilize electron density as a variable, paving the way for subsequent developments. Following this, the *H-F method* emerges as a more sophisticated approximation, grounded in the self-consistent field approach. This method hinges on assumptions aligned with the independent particle approximation and the Pauli exclusion principle. Its framework finds considerable utility in the realm of atoms and molecules, hence extensively employed in quantum chemistry. However, its accuracy diminishes when applied to solids[10].

In our discussion, we will delve into a more contemporary and robust approach: Density Functional Theory (DFT).

2.3.1 The Theorems of Hohenberg and Kohn

In 1964, Hohenberg and Kohn introduced two fundamental theorems that form the bedrock of Density Functional Theory (DFT), elucidating the relationship between electron density and the external potential. These theorems are as follows[11]:

First theorem: ***"The external potential V(r) is a unique functional of the electron density n(r) i.e F[n(r)]. As a result the total ground state energy E of any system is also unique functional of n(r, E=E[n(r)])."***

Second Theorem: ***"The functional E[n] for the total energy has a minimum equal to that ground state energy at ground state density."***

Expanding upon the aforementioned theorems:

The ground state energy of a system comprising interacting electrons in an external field (Vn($\mathbf{r}$)) can be expressed as a unique functional, denoted as F[n($\mathbf{r}$)], of the single-particle electron density, n($\mathbf{r}$)":

$$E[n(\vec{\mathbf{r}})] = F[n(\vec{\mathbf{r}})] + \int V(\vec{\mathbf{r}})n(\vec{\mathbf{r}})\, d^3r \tag{2.4}$$

$$F[n(\vec{\mathbf{r}})] = T_0[n] + \frac{1}{2}\iint \frac{e^2}{4\pi\epsilon_0}\frac{n(\vec{\mathbf{r}'})n(\vec{\mathbf{r}})}{|\vec{r}-\vec{r'}|}\, d^3r\, d^3r' + E_{XC}[n] \tag{2.5}$$

Where $T_0[n]$ is the kinetic energy of non-interacting electrons , the senond term is the classical coulomb energy and E_{XC} exchange correlation energy. The functional $E[n(\vec{\mathbf{r}})]$ is minimum at the equilibrium density $n_0(\vec{r})$ according to the variation $\delta n(\vec{r})$:

$$\left.\frac{\delta E[n(\vec{\mathbf{r}})]}{\delta n(\vec{\mathbf{r}})}\right|_{n=n_0} \tag{2.6}$$

Understanding the properties of ground-state density $n_0(\vec{r})$ in a multi electron system:

1."A direct implication of the one-to-one correspondence between the ground-state density $n_0(\vec{r})$ of a many-electron system (such as an atom, molecule, or solid) and the external potential V_{ext} is the uniqueness of the ground-state expectation value of any observable $\hat{O}$. This implies that the expectation value of any observable in the ground state is solely determined by the exact ground-state electron density. "

$$< \Psi|\hat{O}|\Psi >= O[\rho] \tag{2.7}$$

2."For $\hat{O}$ being the hamiltonian $\hat{H}$, the ground-state total energy functional $H[\rho] = E_{V_{ext}}[\rho]$ is of the form"

$$\begin{aligned} E_{V_{ext}}[\rho] &= \underbrace{< \Psi|\hat{T} + \hat{V}|\Psi >}_{F_{HK}[\rho]} + < \Psi|\hat{V_{ext}}|\Psi > \\ &= F_{HK}[\rho] + \int \rho(\vec{r}) V_{ext}(\vec{r}) d\vec{r} \end{aligned} \tag{2.8}$$

Here $F_{HK}[\rho]$represents the Hohenberg-Kohn density functional, which exhibits a **universal** nature applicable to any multi-electron system. The functional $E_{V_{ext}}[\rho]$ achieves its minimum value, equivalent to the ground-state total energy, when evaluated for the ground-state density corresponding to the external potential V_{ext} .

We will examine three fundamental consequences of the Hohenberg-Kohn density functional l $F_{HK}[\rho]$: invertibility (establishing a one-to-one correspondence $\rho \leftrightarrow V_{ext}$),universality, and the variational property (minimal value).

Firstly, for a given many-electron system, there exists a singular external potential V_{ext} , and solving the Hamiltonian equation (2.2) and Schrödinger's equation for this specific V_{ext} leads to a unique ground-state wave function for the many-particle system. From this wave function, we can straightforwardly compute the corresponding

electron density. The first theorem of Hohenberg and Kohn guarantees the uniqueness of this calculated electron density for the given V_{ext} and vice-versa.It's essential to note that the density encapsulates as much information as the wave function, not less. All observable quantities can be uniquely derived from the density alone, expressed as functionals of the density. This establishes the one-to-one correspondence between the electron density ρ and and the external potential V_{ext}.

Second, the universality of $F_{HK}[\rho]$ arises from its independence regarding information on the nuclei and their positions. As a result, $F_{HK}[\rho]$ serves as a universal functional applicable to any many-electron system. The functional form of $F_{HK}[\rho]$ is expressed as:

$$F[n(r)] = T_0[n] + \frac{1}{2}\frac{e^2}{4\pi\epsilon_0}\iint \frac{n(r)n(r')}{|r-r'|}d^3r d^3r' + E_{XC}[n] \tag{2.9}$$

Here, the first term denotes the kinetic energy of a non-interacting electron gas of density n[r]. The second term represents the classical Coulomb energy, while the third term accounts for the exchange-correlation energy. Consequently, an expression for $F_{HK}[\rho]$ exists in principle, applicable to every conceivable atom, molecule, or solid. This universality underscores the versatility and broad applicability of the Hohenberg-Kohn density functional[12].

Thirdly, the second theorem facilitates the utilization of the variational principle, such as the Rayleigh-Ritz method, to determine the ground-state density. Out of the infinite potential densities, the one that minimizes the functional $E_{V_{ext}}[\rho]$ corresponds to the ground-state density for the external potential $V_{ext}(\vec{r})$. This process relies on the approximate knowledge of $F_{HK}[\rho]$. By employing this theorem, one can efficiently identify the ground-state density, a crucial step in understanding the electronic structure and properties of complex systems[13].

2.3.2 The Kohn-Sham equation

The equations formulated by Kohn and Sham in 1965 marked a pivotal moment, transforming Density Functional Theory (DFT) into a practical computational tool [2]. They introduced two key energy functionals, $E_e[\rho]$ and $E_{HF}[\rho]$ associated with the exact and Hartree-Fock Hamiltonians, respectively.

$$E_e = T + V \tag{2.10}$$

$$E_{HF} = T_0 + \underbrace{V_H + V_x}_{\text{V}} \tag{2.11}$$

where T is the exact (true) kinetic energy functional and V is exact electron-electron potential energy functional , T_0 is the kinetic energy functional for the non-interacting electron gas, V_H is the Hartree contribution and V_x is the exchange contribution. The functional for the correlation contribution is:

$$V_c = T - T_0 \tag{2.12}$$

The fraction of total energy present in the Hartree-Fock solution but absent in the Hartree solution constitutes the exchange contribution. The Hartree functional, is given by:

$$E_H = T_0 + V_H \tag{2.13}$$

It can be written as

$$V_x = V - V_H \tag{2.14}$$

Now rewriting the Hohenberg-Kohn functional from the above idea:

$$\begin{aligned} F_{HK} &= T + V + T_0 + T_0 \\ &= T_0 + V + \underbrace{(T - T_0)}_{\text{Vc}} \\ &= T_0 + V + V_c + V_H - V_H \\ &= T_0 + V_H + V_c + \underbrace{(V - V_H)}_{\text{Vx}} \\ &= T_0 + V_H + \underbrace{V_x + V_C}_{\text{Vxc}} \end{aligned}$$

Here The V_{XC} is the exchange-correlation energy fuctional . Assuming we know V_{XC} , we can explicitly write the energy functional:

$$E_{V_{ext}}[\rho] = T_0[\rho] + V_H[\rho] + V_{xc}[\rho] + V_{ext}[\rho] \tag{2.15}$$

So, the expression can be interpreted as the energy functional of a non-interacting classical electron gas influenced by two external potentials: one arising from the nuclei and the other stemming from the exchange-correlation effect. The corresponding Hamiltonian, known as the Kohn-Sham Hamiltonian, is formulated as:

$$\hat{H_{KS}} = \hat{T_0} + \hat{V_H} + \hat{V_{xc}} + \hat{V_{ext}} \tag{2.16}$$

i.e,

$$\hat{H_{KS}} = -\frac{\hbar^2}{2m_e}\vec{\nabla_i^2} + \frac{e^2}{4\pi\epsilon_0}\int \frac{\rho(\vec{r'})}{|\vec{r} - \vec{r'}|}d\vec{r'} + V_{xc} + V_{ext} \tag{2.17}$$

Where the exchange -correlation potential is given by the functional derivative ,

$$\hat{Vxc} = \frac{\delta V_{xc}}{\delta \rho} \tag{2.18}$$

The K-S equation in the eigen value form:

$$\left[-\frac{\hbar^2}{2m_e}\nabla^2 + V_{ext}(\vec{r}) + V_H(\vec{r}) + V_{xc}(\vec{r})\right]\phi_i(\vec{r}) = \epsilon_i\phi_i(\vec{r}) \tag{2.19}$$

i.e,

$$\left[-\frac{\hbar^2}{2m_e} + V_{eff}\right]\phi_i(\vec{r}) = \epsilon_i\phi_i(\vec{r}) \tag{2.20}$$

This equation is known as the Kohn-Sham equation and $\phi_i(\vec{r})$ is the Kohn-Sham states, ϵ_i is the Kohn-Sham energy, and V_{eff} is the Kohn-Sham potential.

So the exact ground state density $\rho(\vec{r})$ of an N- electron system from single particle is

$$\rho(\vec{r}) = \sum_{i=1}^{N} \phi_i(\vec{r}) * \phi_i(\vec{r}) \tag{2.21}$$

It's crucial to note that the single-particle wave functions ϕ_i do not represent the wave functions of individual electrons; instead, they describe mathematical quasi-particles lacking direct physical interpretation. However, the aggregate density of these quasi-particles is ensured to match the true electron density. Similarly, the single-particle energies ϵ_i should not be misconstrued as energies pertaining to individual electrons[14].

Both the Hartree operator V_H and the exchange-correlation operator V_{xc} depend on the density $\rho(\vec{r})$, which, in turn, is dependent on the single-particle wave functions ϕ_i being sought. This dependence creates a self-consistency problem, as we're stuck in a loop: the solutions (ϕ_i) determine the original equation(V_H and V_{xc} in H_{KS}),yet the equation cannot be formulated and solved until its solution is known. To overcome this challenge, a self-consistent method is employed, iteratively carried out on a computer as depicted in Figure 2.1[15].

Initially, an educated guess is made regarding the form of the single-particle wave functions $\phi_i(\vec{r})$ from which an initial electron density $\rho(\vec{r})$ is constructed. This constructed density is then utilized to formulate the Kohn-Sham Hamiltonian (H_{KS}). Solving the eigenvalue problem yields a new set of single-particle wave functions (ϕ_i) from which a new electron density ($\rho(\vec{r'})$) is determined.This iterative process is repeated until the density converges, ensuring consistency with the Hamiltonian.

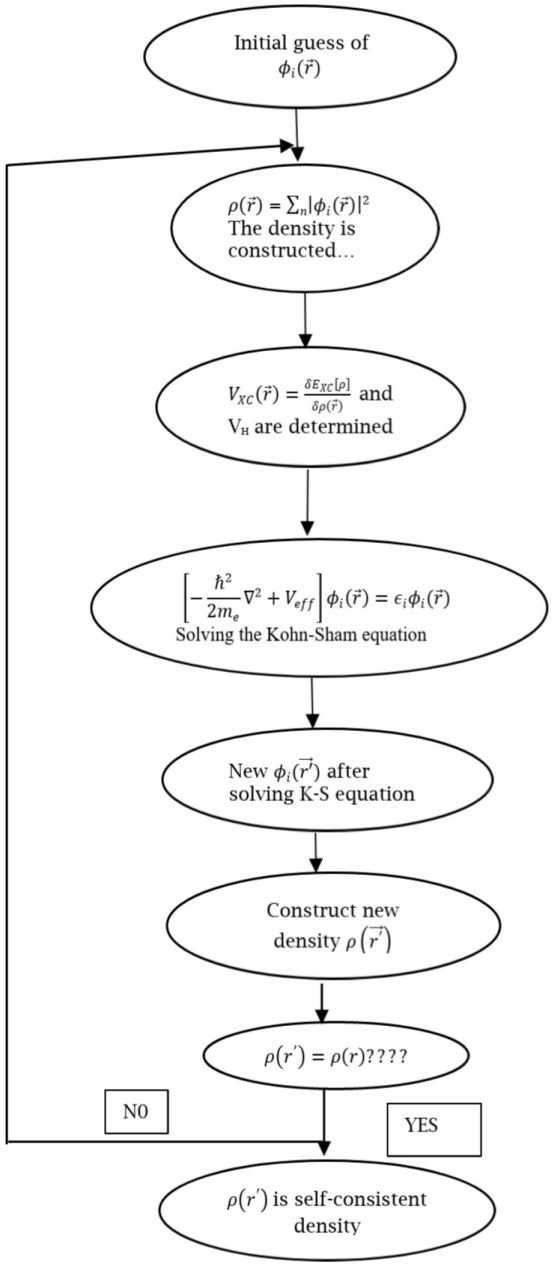
Initial guess of $\phi_i(\vec{r})$
$\rho(\vec{r}) = \sum_n |\phi_i(\vec{r})|^2$ The density is constructed...
$V_{XC}(\vec{r}) = \frac{\delta E_{XC}[\rho]}{\delta \rho(\vec{r})}$ and V_H are determined
$\left[-\frac{\hbar^2}{2m_e}\nabla^2 + V_{eff}\right]\phi_i(\vec{r}) = \epsilon_i \phi_i(\vec{r})$ Solving the Kohn-Sham equation
New $\phi_i(\vec{r'})$ after solving K-S equation
Construct new density $\rho(\vec{r'})$
$\rho(r') = \rho(r)????$
N0
YES
$\rho(r')$ is self-consistent density

Figure 2.1: Flow chart for the scf calculation to solve Kohn-Sham equations.

2.3.3 The exchange-correlation functional

The primary challenge posed by Equation 2.19 is the lack of exact knowledge regarding the exchange-correlation potential V_{xc} or the corresponding exchange-correlation energy (E_{xc}).However, various approximations have been developed to address this issue, such as the Local Density Approximation (LDA), Generalized Gradient Approximation (GGA), meta-GGA, Hybrid-functional, and RPA/GW methods. For the scope of our discussion, we will focus on GGA and LDA[16].

The efficacy of Density Functional Theory (DFT) crucially hinges on the accuracy of the exchange-correlation functional employed to solve the Hamiltonian. Therefore, the choice of approximation method greatly impacts the quality of DFT predictions.

Local Density Approximation

A commonly utilized approximation in Density Functional Theory (DFT) is the Local Density Approximation (LDA). In LDA, it is assumed that the exchange-correlation energy density at each position within a molecule is equivalent to that of a Uniform Electron Gas (UEG) with the same density as observed at that position[17]. Mathematically, this is expressed as:

$$E_{xc}^{LDA}[\rho] = E_{x}^{LDA}[\rho] + E_{c}^{LDA}[\rho] \tag{2.22}$$

The expression for exchange energy is simple

$$E_{x}^{LDA}[\rho] = C \int \rho^{\frac{4}{3}}(\vec{r}) d\vec{r} \tag{2.23}$$

Various expressions for the correlation energy $E_{xc}^{LDA}[n]$ have been derived by fitting to the outcomes of accurate Quantum Monte Carlo (QMC) calculations for the UEG. Thus, the exchange-correlation functional takes the form:

$$E_{xc}^{LDA}[\rho] = \int \rho(\vec{r}) \epsilon_{xc}(\rho(\vec{r})) d\vec{r} \tag{2.24}$$

Generalised Gradient Approximation

An enhancement in accuracy beyond that provided by LDA can be achieved through Generalized Gradient Approximation (GGA) functionals. Unlike LDA, GGA functionals depend not only on the value of the electron density at a point but also on its gradient. Therefore, we have:

$$E_{xc}^{GGA}[\rho] = \int \rho(\vec{r})\epsilon_{xc}(\rho(\vec{r}), |\nabla\rho(\vec{r})|)d\vec{r} \tag{2.25}$$

Most GGA functionals are formulated as a correction term added to the LDA functional:

$$\epsilon_{x/c}^{GGA}[\rho] = \epsilon_{x/c}^{LDA}[\rho] + \Delta\epsilon_{x/c}\left[\frac{|\nabla\rho(\vec{r})}{\rho^{4/3}(\vec{r})}\right] \tag{2.26}$$

2.3.4 Spin-Orbit Interaction

Spin-orbit coupling (SOC) refers to the interaction between an electron's spin magnetic moment and its orbital angular momentum. In solids, SOC leads to the lifting of degeneracy among one-electron levels. This effect is particularly pronounced in materials containing heavy elements such as **Pb**, **I**, or **Bi**, where relativistic effects significantly influence electron behavior. Consequently, solving the relativistic Dirac equation becomes necessary to accurately account for SOC.

However, as an initial approximation, the non-relativistic Kohn-Sham equation can be employed by introducing a spin-dependent term in the Hamiltonian:

$$\left[-\frac{1}{2}\nabla^2 + V_{ext}(\mathbf{r}) + V_H(\mathbf{r}) + V_{xc}(\mathbf{r}) + \mu_B\sigma.B_{xc}(\mathbf{r})\right]\phi_i(\mathbf{r}) = \epsilon_i\phi_i(\mathbf{r}) \tag{2.27}$$

where μ_B is the Bohr magneton, B_{xc} is the exchange and correlation magnetic field, and σ is the matrix vector defined by:

$$\sigma = \sigma_x u_x + \sigma_y u_y + \sigma_z u_z \tag{2.28}$$

Where $\sigma_x, \sigma_y, \sigma_z$ are Pauli matrices and u_x, u_y, u_z are the unit vectors along the x, y

and z direction.The spin calculations can be conducted in either a collinear or non-collinear manner. The collinear approach assumes that spin densities align in the same direction. To incorporate SOC effects, a non-collinear spin calculation can be performed using packages like Quantum ESPRESSO (QE)[4].

2.4 Solving the equations

In either the approximation of Hartree-Fock (HF) or Density Functional Theory (DFT), the result yields an infinite sequence of one-electron equations of the following form (where m is an integer that counts the members of the set):

$$\underbrace{\left[-\frac{\hbar^2}{2m_e}\vec{\nabla}_m^2 + \frac{e^2}{4\pi\epsilon_0}\int\frac{\rho(\vec{r'})}{|\vec{r}-\vec{r'}|}d\vec{r'} + V_\alpha + V_{ext}\right]}_{H_{sp}}\phi_m(\vec{r}) = \epsilon_m\phi_m(\vec{r}) \tag{2.29}$$

Here the H_{sp} is the single particle Hamiltonian. For Hartree-Fock , V_α is the exchange operator. The ϕ_m are true one-electron (or single-particle) orbitals for HF. In HF, the exchange is treated exactly, but correlation effects are not incorporated at all[4].

For DFT, V_α represents the exchange-correlation operator , which is approximated in methods like LDA, GGA, or others. In DFT, both exchange and correlation effects are treated, albeit approximately. The ϕ_m represent mathematical quasi single-particle orbitals. The resemblance between the Hartree-Fock and Kohn-Sham equations allows for the use of similar mathematical techniques to solve them. Typically, "solving" entails finding the coefficients c_p^m needed to express ϕ_m in a given basis set ϕ_p^b :

$$\phi_m = \sum_{p=1}^{P} c_p^m \phi_p^b \tag{2.30}$$

The wave functions ϕ_m are theoretically infinite, as m belongs to a function space with infinite dimensions. Thus, P is infinite. In practice, only a limited number of basis functions are employed. Although such a restricted basis may not perfectly represent ϕ_m, it is still possible to construct a basis that can generate a function that

closely resembles ϕ_m. Substituting over two conditions, we get:

$$\begin{bmatrix} ... & ... & ... \\ | & \langle \phi_i^b | \hat{H} | \phi_j^b \rangle - \epsilon_m \langle \phi_i^b | \phi_j^b \rangle & | \\ ... & ... & ... \end{bmatrix} \begin{bmatrix} c_1^m \\ | \\ c_P^m \end{bmatrix} = \begin{bmatrix} 0 \\ | \\ 0 \end{bmatrix}$$

Diagonalizing the Hamiltonian matrix will yield P eigenvalues and P sets of coefficients for each of the P eigenfunctions in the specified basis (for more eigenfunctions). The larger P, the better the eigenfunction approximation, but it also increases the computational complexity of matrix diagonalization on classical computers[4].

2.5 Applications of DFT

2.5.1 Equilibrium Structure

Atomic forces

In standard DFT, the nuclei are treated as classical particles, allowing us to utilize Newton's equations for their dynamics. The total force acting on each atom can be determined using classical mechanics:

$$F_I = -\frac{\partial U}{\partial R_I} \tag{2.31}$$

where F_I is the force on I-th nucleus and U is the total potential energy. However, directly calculating $\frac{\partial U}{\partial R_I}$ is challanging. Although the finite displacement method is an option, it's highly time-consuming. Alternatively, the Hellmann-Feynman theorem offers a solution by employing first-order perturbation theory:

$$F_I = -\langle \Psi | \frac{\partial H}{\partial R_I} | \Psi \rangle - \frac{\partial V_{NN}}{\partial R_I} \tag{2.32}$$

where V_{NN} is the classical potential energy of nuclei. The second term in Eq. 2.32 accounts for the electrostatic field of the nuclei.

Ionic Optimization

Once the atomic forces on each atom are established, structural optimization can proceed using various algorithms such as conjugate gradient (CG), quasi-Newton, and damped molecular dynamics. The equilibrium structure can be attained by initiating with an initial guess of atomic positions, followed by computing the electron density and energy through Kohn-Sham self-consistent calculations. This step is known as the electronic step. Subsequently, the atomic force on each atom can be determined using Equation 2.32. New atomic positions can then be obtained employing an algorithm like CG. These updated atomic positions serve as a new starting point for the cycle, referred to as the ionic step. The termination condition for the loop can be chosen based on either the atomic forces and stress or the energy of the entire structure[18].

2.5.2 Band Structures and Density of States (DOS)

After solving the periodic Kohn-Sham equation (Eq. 2.20), the energy states, known as Kohn-Sham states, can be obtained. The total energy from Eq. 2.20 is given by:

$$E = \frac{1}{\Omega_{BZ}} \sum_{n} \int_{BZ} f_{n\mathbf{k}} \epsilon_{n\mathbf{k}} d\mathbf{k} - \int V_{xc}(\mathbf{r}) n(\mathbf{r}) d\mathbf{r} - E_H + E_{xc} \tag{2.33}$$

Here, the first term represents the band structure energy, and the subsequent terms account for the double counting inherent in the first term. The electronic density of states (DOS) can be calculated as:

$$\rho(E) = \frac{1}{\Omega} \sum_{n} \int_{BZ} d\mathbf{k} \delta(E - \epsilon_{n\mathbf{k}}) \tag{2.34}$$

where $\rho(E)dE$ denotes the number of Kohn-Sham states between energy levels E and E+dE. The band structure and DOS are valuable tools for analyzing the

electronic structure. Additionally, besides the total DOS, partial density of states can be determined for each orbital.

2.6 Computational Package

2.6.1 VASP

VASP (Vienna Ab-initio Simulation Package) is a computational simulation tool that employs Density Functional Theory (DFT) to provide a diverse array of material properties, such as total energy, electronic density of states, band structure, and lattice parameters. One of the primary benefits of utilizing VASP is its capability to deliver highly accurate electronic structures. Additionally, VASP boasts scalability, enabling its utilization across a broad spectrum of computer systems, ranging from small-scale to large-scale computing platforms.

INPUT FILES

To initiate a calculation in VASP, a set of input files is necessary to compute various properties associated with the material under investigation.

The essential input files for running a VASP calculation include:

1. INCAR - This file contains critical settings for the VASP calculation, encompassing parameters like calculation type, convergence criteria, and electronic configurations.

2. POSCAR - This file encapsulates the crystal structure of the material being simulated, detailing atomic positions and lattice vectors.

3. POTCAR - This file holds the pseudopotentials utilized to characterize the electron-ion interactions within the material.

4. KPOINTS - This file delineates the k-point sampling utilized in the calculation.

Accurate and reliable calculations hinge upon the meticulous setup of these input files. VASP offers a plethora of tools and comprehensive documentation to aid users in configuring input files accurately.

OUTPUT FILES

When conducting a calculation with VASP, several output files are generated, each providing valuable information about the computation:

1. OUTCAR - This file furnishes comprehensive details regarding the calculation, encompassing convergence criteria, the number of electronic and ionic steps taken, and the final total energy attained.

2. OSZICAR - This file offers a condensed summary of the ionic steps taken during the calculation, along with the final total energy achieved.

3. vasprun.xml - This XML-formatted file presents an overview of the entire computation, featuring crucial data such as the total energy, electronic density of states, and band structure.

4. CHG, CHGCAR - These files contain the charge density distribution of the system, which can be visualized using specialized visualization software to gain insights into the electronic structure.

5. WAVECAR - This file holds the wavefunctions of the system, allowing for the calculation of additional properties or the resumption of a calculation from a specific point.

In addition to these primary output files, VASP may generate various other files depending on the specific nature of the computation being performed. For instance, in phonon calculations, a FORCE CONSTANTS file may be produced, detailing the

force constants of the system.

2.6.2 LAMMPS

LAMMPS (Large-scale Atomic/Molecular Massively Parallel Simulator) is a powerful molecular dynamics simulation software capable of simulating a wide range of materials and systems at the atomic scale. One of the key functionalities of LAMMPS is its ability to perform relaxation simulations, which are essential for studying the equilibrium structures and properties of materials under various conditions.

LAMMPS, stands out for its comprehensive capabilities in atomistic simulations. Treating each atom as an individual entity, it meticulously models interatomic interactions using a diverse array of potential models, from classical force fields like Lennard-Jones and Tersoff potentials to specialized ones tailored for specific materials and applications. Its high degree of parallelization enables efficient utilization of computational resources across multiple processors or computing nodes, facilitating simulations of large-scale systems and expediting relaxation calculations. LAMMPS excels in dynamical relaxation simulations, guiding systems through iterative energy minimization and molecular dynamics steps until reaching equilibrium, thereby offering invaluable insights into structural and thermodynamic properties.

2.6.3 SIESTA

SIESTA (Spanish Initiative for Electronic Simulations with Thousands of Atoms) is a widely used computational simulation tool based on Density Functional Theory (DFT) for studying the electronic structure of materials. Developed by the Spanish National Research Council (CSIC), SIESTA provides an efficient and accurate approach to investigate a variety of material properties, including total energy, electronic density of states, band structure, and atomic forces. SIESTA is recognized for its efficiency in handling large-scale simulations involving thousands of atoms, making it suitable for studying systems with complex structures or interfaces. It offers

flexibility in choosing the level of theory and the type of basis sets, allowing users to tailor simulations according to their specific research needs. SIESTA employs localized atomic orbitals as basis sets, resulting in computational efficiency and enabling simulations of systems with high precision. Additionally, SIESTA is parallelized, enabling efficient utilization of computational resources across multiple processors or computing nodes, thereby reducing the simulation time for large-scale calculations.

INPUT FILES

Similar to VASP, initiating a simulation in SIESTA requires a set of input files, including:

1. Input File (input.fdf): This file contains parameters for the simulation, such as calculation type, convergence criteria, and system setup details.
2. Pseudopotential Files (input.psf) : SIESTA utilizes pseudopotentials to approximate the electron-ion interactions within the material, which are specified in separate files.

OUTPUT FILES

Upon completion of a simulation, SIESTA generates several output files, including:

1. Output Log File: This file provides detailed information about the simulation process, including convergence criteria, the number of electronic and ionic steps, and the final total energy.
2. Electronic Density File: SIESTA produces files containing electronic density distributions, which can be visualized to analyze the electronic structure of the material.
3. Band Structure and Density of States Files: SIESTA generates files containing

information about the electronic band structure and density of states, facilitating analysis of the material's electronic properties.

4. Force and Stress Files: SIESTA provides files containing information about atomic forces and stresses, which are crucial for understanding mechanical and structural properties.

Generation of SIESTA Input Files through Iterative Visualization Processes

For generating SIESTA input files we have used a sequential process involving multiple visualization tools. Beginning with a relaxed structure obtained from LAMMPS simulations, the lammps.dat.min file is subjected to visualization in OVITO software for initial analysis. Subsequently, the structure is exported as a .cif file for further refinement in Burai, where adjustments are made to ensure proper centering of layer in z direction. Following this, the centered structure is exported once more as a POSCAR file and imported into WXDragon for the finalization of the SIESTA input file. This iterative approach harnesses the capabilities of each visualization tool to refine the atomic structure iteratively, culminating in the creation of an accurate and optimized SIESTA input file for subsequent computational simulations.

RESULTS AND DISCUSSIONS

Chapter 3

Results and discussions

3.1 Structural relaxation using VASP

We have used Vienna Ab initio Simulation Package(VASP) for the relaxation of band structures of different 2D materials, substitutionally doped 2D materials and NH_3 adsorbed doped 2D materials.

3.1.1 POSCAR FILE FOR MoS_2

(atomic position)

```
12 atoms
2 atom types

1.0000000000
     6.368133068    0.0000000000    0.0000000000
    -3.1840672684    5.5149645877    0.0000000000
     0.0000000000 0.0000000000    18.1271132423
```

INCAR FILE FOR MoS_2

3.1.2 POSCAR FILE FOR WSe_2

atomic positions

```
12 atoms
2 atom types

1.0
        9.9570198059          0.0000000000          0.0000000000
       -4.9785110512          8.6230314350          0.0000000000
        0.0000000000          0.0000000000         18.3585529327
```

3.1.3 POSCAR FILE FOR Au DOPED MoS_2

```
"Mo1 S2"
1.0
        9.5521993637          0.0000000000          0.0000000000
       -4.7761007834          8.2724466750          0.0000000000
        0.0000000000          0.0000000000         18.1271133423
   Mo    S   Au
    9   17    1
Cartesian
     0.000000000          0.000000000          9.063556671
    -1.592033642          2.757482307          9.063556671
    -3.184067284          5.514964614          9.063556671
```

```
 3.184066549          0.000000000          9.063556671
 1.592032908          2.757482307          9.063556671
-0.000000734          5.514964614          9.063556671
 6.368133099          0.000000000          9.063556671
 4.776099457          2.757482307          9.063556671
 3.184065815          5.514964614          9.063556671
 1.592033117          0.919160749         10.627113246
-0.000000490          3.676642994         10.627113246
-1.592034131          6.434125301         10.627113246
 4.776099809          0.919160749         10.627113246
 1.592032560          6.434125301         10.627113246
 7.960166073          0.919160749         10.627113246
 6.368132467          3.676642994         10.627113246
 4.776098825          6.434125301         10.627113246
 1.592033117          0.919160749          7.500000096
-0.000000490          3.676642994          7.500000096
-1.592034131          6.434125301          7.500000096
 4.776099809          0.919160749          7.500000096
 3.184066202          3.676642994          7.500000096
 1.592032560          6.434125301          7.500000096
 7.960166073          0.919160749          7.500000096
 6.368132467          3.676642994          7.500000096
 4.776098825          6.434125301          7.500000096
 3.184066202          3.676642994         10.627113246
```

INCAR FILE FOR Au DOPED MoS_2

```
Global Parameters
NCORE  = 4
ISTART =  0          (Read existing wavefunction, if there)
```

```
ISPIN  =  1            (Non-Spin polarised DFT)
ICHARG =  2         (Non-self-consistent: GGA/LDA band structures)
LREAL  = .FALSE.       (Projection operators: automatic)
ENCUT  = 520       (Cut-off energy for plane wave basis set, in eV)
 when perform structure lattice relaxation calculation)
LWAVE  = .TRUE.        (Write WAVECAR or not)
LCHARG = .TRUE.        (Write CHGCAR or not)
ADDGRID= .TRUE.        (Increase grid, helps GGA convergence)
LASPH  = .TRUE.        (Give more accurate total energies )
PREC   = Accurate      (Accurate strictly avoids any aliasing)
LVTOT  = .TRUE.      (Write total electrostatic potential into LOCPOT or not)
 KPAR   = 2           (Divides k-grid into separate groups)
 NGXF    = 300        (FFT grid mesh density for nice charge/potential plots)
 NGYF    = 300        (FFT grid mesh density for nice charge/potential plots)
 NGZF    = 300        (FFT grid mesh density for nice charge/potential plots)
 #NELECT = 78
Static Calculation
ISIF = 2
GGA = PE
ISMEAR =  0            (gaussian smearing method)
SIGMA  =  0.05         (please check the width of the smearing)

NELM   =  90          (Max electronic SCF steps)
EDIFF  =  1E-06      (SCF energy convergence, in eV)
IBRION = 2
NSW =99
EDIFFG = -0.002
IVDW  = 11
```

3.1.4 POSCAR FILE FOR NH_3 ADSORBED Au DOPED MoS_2

```
    "Mo1 S2"
1.0
        9.5521993637         0.0000000000         0.0000000000
       -4.7761007834         8.2724466750         0.0000000000
        0.0000000000         0.0000000000        18.1271133423
   Mo    S   Au    H    N
    9   17    1    3    1
selective dynamics
Cartesian
     0.000000000         0.000000000         9.063556131 F F F
    -1.592033357         2.757481814         9.063556131 F F F
    -3.184067284         5.514964614         9.063556131 F F F
     3.184066549         0.000000000         9.063556131 F F F
     1.592032908         2.757481814         9.063556131 F F F
    -0.000001019         5.514964614         9.063556131 F F F
     6.368131960         0.000000000         9.063556131 F F F
     4.776098603         2.757481814         9.063556131 F F F
     3.184065815         5.514964614         9.063556131 F F F
     1.592032868         0.919160933        10.627112166 F F F
    -0.000000063         3.676642748        10.627112166 F F F
    -1.592033704         6.434124315        10.627112166 F F F
     4.776099702         0.919160933        10.627112166 F F F
     1.592032560         6.434124315        10.627112166 F F F
     7.960165397         0.919160933        10.627112166 F F F
     6.368131471         3.676642748        10.627112166 F F F
     4.776098825         6.434124315        10.627112166 F F F
     1.592032868         0.919160933         7.499999556 F F F
    -0.000000063         3.676642748         7.499999556 F F F
```

```
   -1.592033704        6.434124315        7.499999556 F F F
    4.776099702        0.919160933        7.499999556 F F F
    3.184065775        3.676642748        7.499999556 F F F
    1.592032560        6.434124315        7.499999556 F F F
    7.960165397        0.919160933        7.499999556 F F F
    6.368131471        3.676642748        7.499999556 F F F
    4.776098825        6.434124315        7.499999556 F F F
    3.184065775        3.676642748       10.627112166 F F F
    4.544491094        3.634130700       13.510810609 T T T
    4.087431497        4.500030277       12.187849820 T T T
    3.221530569        3.177069729       12.644910395 T T T
    3.736953574        3.984607569       12.995387898 T T T
```

3.1.5 RELAXED POSCAR (CONTCAR) FILE FOR NH_3 ADSORBED Au-DOPED MoS_2

```
"Mo1 S2"
   1.00000000000000
     9.5521993636999998    0.0000000000000000    0.0000000000000000
    -4.7761007834000004    8.2724466749999994    0.0000000000000000
     0.0000000000000000    0.0000000000000000   18.1271133422999995
   Mo   S    Au   H    N
     9    17     1     3     1
Direct
  0.0000000000000000  0.0000000000000000  0.4999999702020972
  0.0000000000183888  0.3333332836503260  0.4999999702020972
  0.9999999999600959  0.6666666864915172  0.4999999702020972
  0.3333333432193655  0.0000000000000000  0.4999999702020972
  0.3333333135063796  0.3333332836503260  0.4999999702020972
  0.3333333134480867  0.6666666864915172  0.4999999702020972
  0.6666665673038636  0.0000000000000000  0.4999999702020972
```

```
0.6666665673222454  0.3333332836503260  0.4999999702020972
0.6666666865035111  0.6666666864915172  0.4999999702020972
0.2222222089873114  0.1111111342400974  0.5862550735643808
0.2222222536631975  0.4444444180113152  0.5862550735643808
0.2222222090211332  0.7777776718034843  0.5862550735643808
0.5555555820427358  0.1111111342400974  0.5862550735643808
0.5555555224044326  0.7777776718034843  0.5862550735643808
0.8888888358586087  0.1111111342400974  0.5862550735643808
0.8888887763700026  0.4444444180113152  0.5862550735643808
0.8888888358924234  0.7777776718034843  0.5862550735643808
0.2222222089873114  0.1111111342400974  0.4137448370501744
0.2222222536631975  0.4444444180113152  0.4137448370501744
0.2222222090211332  0.7777776718034843  0.4137448370501744
0.5555555820427358  0.1111111342400974  0.4137448370501744
0.5555555224494455  0.4444444180113152  0.4137448370501744
0.5555555224044326  0.7777776718034843  0.4137448370501744
0.8888888358586087  0.1111111342400974  0.4137448370501744
0.8888887763700026  0.4444444180113152  0.4137448370501744
0.8888888358924234  0.7777776718034843  0.4137448370501744
0.5555555224494455  0.4444444180113152  0.5862550735643808
0.6954061388605908  0.4393054247158403  0.7453371286354908
0.6998938917828355  0.5439781546854121  0.6723546981724553
0.5292826294600061  0.3840544223272389  0.6975688934151947
0.6320500969617484  0.4816721975424514  0.7169033288755884
```

3.2 Electronic band structures

In two-dimensional (2D) materials, the band structure refers to the distribution of energy levels, or band formed by the allowed electronic states within the material's crystal lattice. These bands represent the energy levels that electrons can occupy

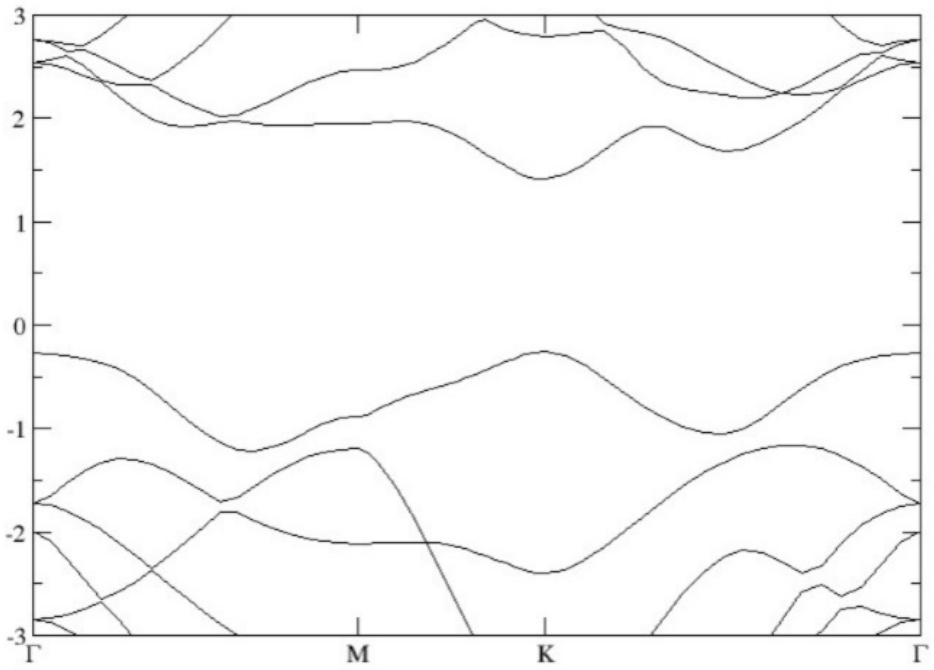

Figure 3.1: Band structure of mono layered MoS_2

in the material, and the band structure provides valuable insights into its electronic properties[10]. Band structure in 2D materials illustrates how energy levels for electrons are distributed across different momentum states within the material's Brillouin zone. It describes the relationship between energy and momentum for electrons, indicating which energy levels are available for electron occupation at different momenta. We can easily observe from Figure 3.1 and Figure 3.2 that the band gap is narrowing when Au is substitutionally doped at the S site in MoS_2. This distortion is causing the conduction band to shift lower in energy or valance band to rise slightly (observed from Figure 3.3).

The band structures are plotted using xmgrace. The band structure of understudied samples like MoS_2, Au-doped MoS_2, NH_3 adsorbed Au-doped MoS_2 are plotted.

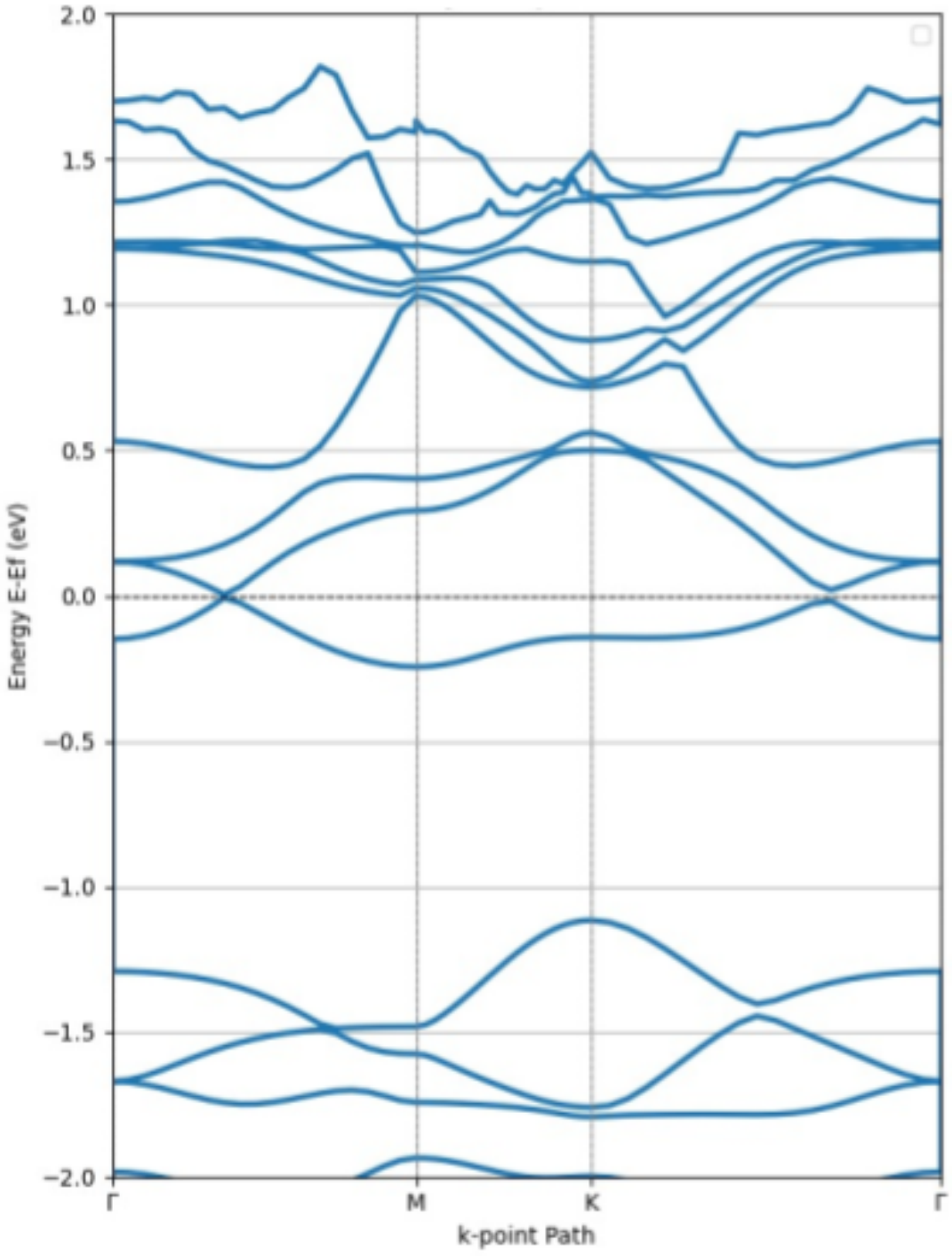

Figure 3.2: Band structure of Au doped mono layered MoS_2

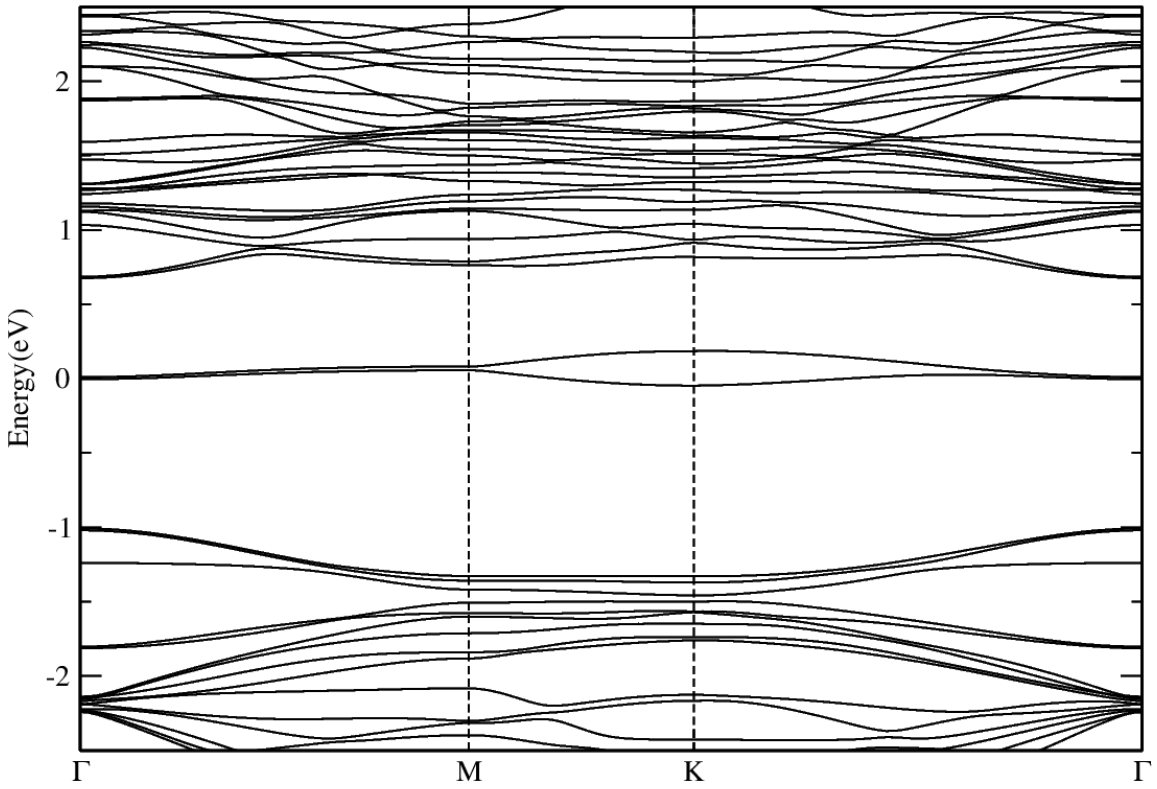

Figure 3.3: Band Structure of NH_3 adsorbed Au doped WSe_2

3.3 Adsorption energy and charge transfer

We got an adsorption energy of -5.452eV when the sensing layer was Au-doped WSe_2. And the charge transfer between the Ammonia gas and the sensing layer we obtained approximately 0.246e.For the calculation of adsorption energy, we referred to equation (1.1), and for charge transfer, we did Bader charge analysis.

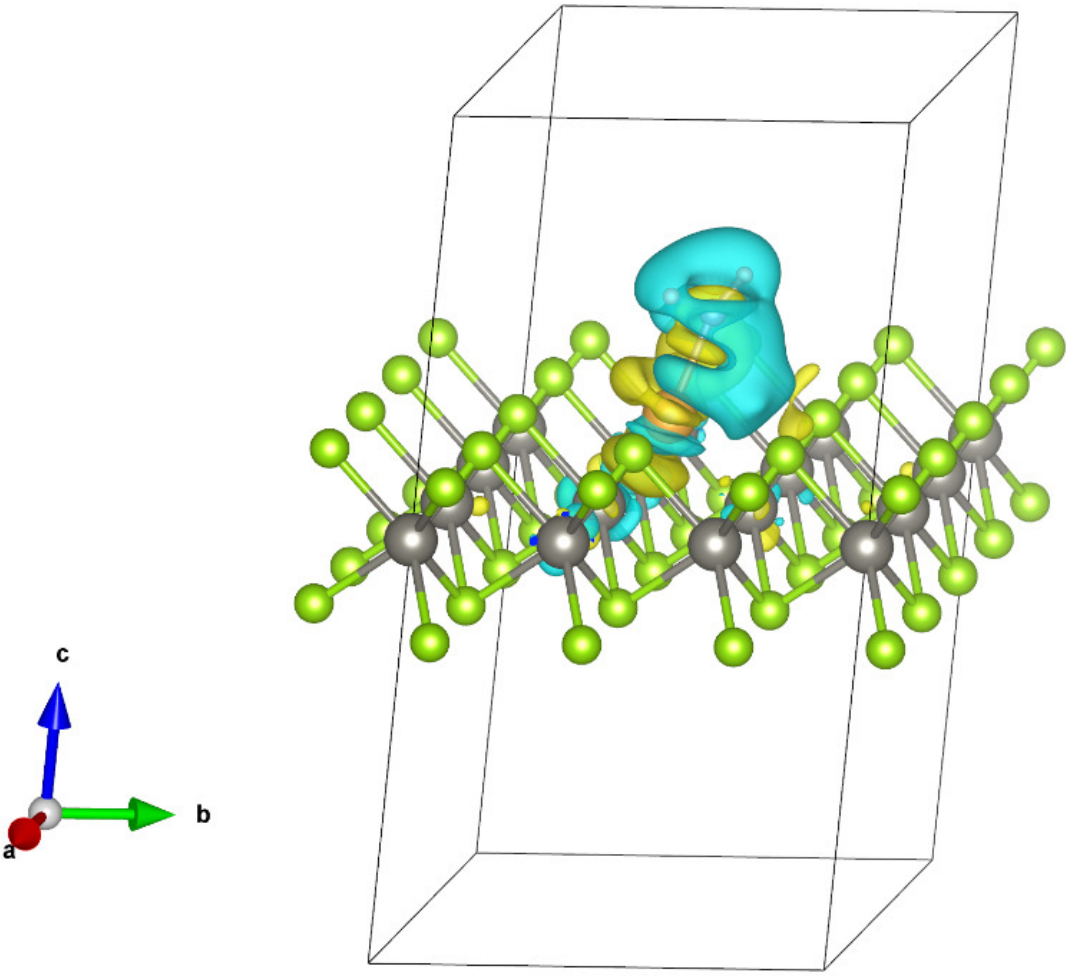

Figure 3.4: Electron density difference of NH_3 adsorbed on Au-doped WSe_2TMD monolayer

SUMMARY AND CONCLUSION

Chapter 4

SUMMARY AND CONCLUSION

4.0.1 Summary

At first, we take some 2D materials to calculate the band structures using VASP. After that, we substitutionally doped MoS_2 and WSe_2, replacing the 'S' atom with 'Au', and again evaluated the band structures. And finally, we absorbed NH_3 gas over the surface of substitutionally doped samples and we calculated adsorption energy and also did bader charge analysis and calculated charge transfer.

4.0.2 Conclusion

Our investigation was focused on analyzing the electronic band structures of the substitutionally doped samples. We also tried to observe how the doped sample responds when NH_3 gas is being adsorbed over the surface of the doped material. We got an adsorption energy of -5.452eV when the sensing layer was Au doped WSe_2. And the charge transfer between the Ammonia gas and sensing layer we obtained approximately 0.246e. These results of adsorption energy and charge transfer indicate that the substitutionally doped WSe_2 monolayer is highly sensitive towards the NH_3 gas.

References

[1] Rousan Debbarma et al. "WS 2-induced enhanced optical absorption and efficiency in graphene/silicon heterojunction photovoltaic cells". In: *Nanoscale* 10.43 (2018), pp. 20218–20225.

[2] Walter Kohn and Lu Jeu Sham. "Self-consistent equations including exchange and correlation effects". In: *Physical review* 140.4A (1965), A1133.

[3] Sanjay Behura et al. "Chemical interaction-guided, metal-free growth of large-area hexagonal boron nitride on silicon-based substrates". In: *ACS nano* 11.5 (2017), pp. 4985–4994.

[4] Evgeny M Alexeev et al. "Resonantly hybridized excitons in moiré superlattices in van der Waals heterostructures". In: *Nature* 567.7746 (2019), pp. 81–86.

[5] Yuan Cao et al. "Unconventional superconductivity in magic-angle graphene superlattices". In: *Nature* 556.7699 (2018), pp. 43–50.

[6] Jonathan S Alden et al. "Strain solitons and topological defects in bilayer graphene". In: *Proceedings of the National Academy of Sciences* 110.28 (2013), pp. 11256–11260.

[7] Chao Ding et al. "Corrugation effect, Dirac cone splitting, and plasmon properties of biased twisted bilayer graphene". In: *Physical Review B* 104.15 (2021), p. 155427.

[8] Humberto R Gutiérrez et al. “Extraordinary room-temperature photoluminescence in triangular WS2 monolayers”. In: *Nano letters* 13.8 (2013), pp. 3447–3454.

[9] Brian Harold Bransden and Charles Jean Joachain. *Physics of atoms and molecules*. Pearson Education India, 2003.

[10] Philip Richard Wallace. “The band theory of graphite”. In: *Physical review* 71.9 (1947), p. 622.

[11] Pierre Hohenberg and Walter Kohn. “Inhomogeneous electron gas”. In: *Physical review* 136.3B (1964), B864.

[12] Yichen Jia et al. “Tunable plasmon–phonon polaritons in layered graphene–hexagonal boron nitride heterostructures”. In: *ACS Photonics* 2.7 (2015), pp. 907–912.

[13] GuangXin Ni et al. “Fundamental limits to graphene plasmonics”. In: *Nature* 557.7706 (2018), pp. 530–533.

[14] Kyle L Seyler et al. “Signatures of moiré-trapped valley excitons in MoSe2/WSe2 heterobilayers”. In: *Nature* 567.7746 (2019), pp. 66–70.

[15] JMB Lopes dos Santos, NMR Peres, and AH Castro Neto. “Graphene bilayer with a twist: electronic structure”. In: *Physical review letters* 99.25 (2007), p. 256802.

[16] Weijiong Chen et al. “Direct observation of van der Waals stacking–dependent interlayer magnetism”. In: *Science* 366.6468 (2019), pp. 983–987.

[17] Guangwei Hu et al. “Topological polaritons and photonic magic angles in twisted α-MoO3 bilayers”. In: *Nature* 582.7811 (2020), pp. 209–213.

[18] Eva Y Andrei and Allan H MacDonald. “Graphene bilayers with a twist”. In: *Nature materials* 19.12 (2020), pp. 1265–1275.

Project2025

ORIGINALITY REPORT

29%	23%	22%	%
SIMILARITY INDEX	INTERNET SOURCES	PUBLICATIONS	STUDENT PAPERS

PRIMARY SOURCES

1	doczz.net Internet Source	1%
2	Al-Sawai, Wael M. "A Study of Topological Insulator States of Half-Heusler Materials and the Momentum Density of Overdoped Cuprates", Proquest, 20111108 Publication	1%
3	Bohuslav Dobias, Hansjoachim Stechemesser. "Coagulation and Flocculation", CRC Press, 2019 Publication	1%
4	dspace.alquds.edu Internet Source	1%
5	hdl.handle.net Internet Source	1%
6	lib.buet.ac.bd:8080 Internet Source	1%
7	Debasree Burman, Himadri Raha, Bibhas Manna, Panchanan Pramanik, Prasanta Kumar Guha. " Substitutional Doping of MoS for Superior Gas-Sensing Applications: A Proof of Concept ", ACS Sensors, 2021 Publication	1%
8	ruor.uottawa.ca Internet Source	1%
9	www.slideshare.net Internet Source	1%

10	pdxscholar.library.pdx.edu Internet Source	1 %
11	etd.aau.edu.et Internet Source	1 %
12	hal.univ-lorraine.fr Internet Source	1 %
13	arxiv.org Internet Source	1 %
14	purehost.bath.ac.uk Internet Source	<1 %
15	Brahmananda Chakraborty. "Electronic Structure and Theoretical Aspects on Sensing Application of 2D Materials", Elsevier BV, 2019 Publication	<1 %
16	blog.vasp.at Internet Source	<1 %
17	m.moam.info Internet Source	<1 %
18	Bai, Haoyun. "Control of Electron and Spin in Two-Dimensional Materials", University of Macau Publication	<1 %
19	Barker, Bradford Alan. "Electronic and Optical Properties of Solids with Strong Spin-Orbit Coupling.", University of California, Berkeley, 2018 Publication	<1 %
20	Denis Misiurev, Vladimír Holcman. "Modeling of Magnetic Films: A Scientific Perspective", Materials, 2024 Publication	<1 %
21	iopscience.iop.org Internet Source	<1 %

22	repository.kaust.edu.sa Internet Source	<1%
23	ccc.keinsci.com Internet Source	<1%
24	Rajendra Prasad. "Electronic Structure of Materials", CRC Press, 2019 Publication	<1%
25	publikationen.ub.uni-frankfurt.de Internet Source	<1%
26	opus.bibliothek.uni-augsburg.de Internet Source	<1%
27	ethesis.nitrkl.ac.in Internet Source	<1%
28	docnum.univ-lorraine.fr Internet Source	<1%
29	Üstündağ, Mehmet. "Bor Bileşiklerinin Yapısal, Elektronik ve Optiksel Özelliklerinin Teorik Olarak Incelenmesi", Sakarya Universitesi (Turkey), 2022 Publication	<1%
30	udspace.udel.edu Internet Source	<1%
31	Fei Lan, Quan Tao, Guangyong Li. "Investigation of electrical properties of contact between Molybdenum disulfide and different metals", 2015 IEEE 15th International Conference on Nanotechnology (IEEE-NANO), 2015 Publication	<1%
32	Jenő Sólyom. "Cohesive Energy of the Electron System", Fundamentals of the Physics of Solids, 2010 Publication	<1%

33	Majid Samadian, Masoud Ajri, Abdolhamid Azizi, Mohammad Amin Hemmatpour-Khotbesara. "Investigating the pinhole effect on the mechanical properties of biphenylene", Applied Physics A, 2023 Publication	<1 %
34	ir.soken.ac.jp Internet Source	<1 %
35	www.pprime.fr Internet Source	<1 %
36	en.wikipedia.org Internet Source	<1 %
37	repository.upenn.edu Internet Source	<1 %
38	uu.diva-portal.org Internet Source	<1 %
39	www.coursehero.com Internet Source	<1 %
40	www.gcwk.ac.in Internet Source	<1 %
41	aip.scitation.org Internet Source	<1 %
42	publications.lib.chalmers.se Internet Source	<1 %
43	Aeberhard, Philippe Christoph. "Computational Modelling of Structure and Dynamics in Lightweight Hydrides.", University of Oxford (United Kingdom) Publication	<1 %
44	core.ac.uk Internet Source	<1 %
45	etd.fcla.edu Internet Source	<1 %

46	fse.studenttheses.ub.rug.nl Internet Source	<1 %
47	June Gunn Lee. "Computational Materials Science - An Introduction", CRC Press, 2019 Publication	<1 %
48	doc.rero.ch Internet Source	<1 %
49	dx.doi.org Internet Source	<1 %
50	www.researchgate.net Internet Source	<1 %
51	L. M. Sandratskii. "Noncollinear magnetism in itinerant-electron systems: Theory and applications", Advances in Physics, 1998 Publication	<1 %
52	Mohamed Khuili, Hajar Saadi, Nejma Fazouan, Yassine Sadiki, Samah Al-Qaisi, El Houssine Atmani, El Hassan Abba. "Study of the dependence of the ZT figure of merit on doping and temperature of ZnO", International Journal of Computational Materials Science and Engineering, 2023 Publication	<1 %
53	Pak, Sarah. "Approximate Time-Dependent Density Functional Theory Methods for Simulating X-Ray Absorption Spectra in Transition Metal Complexes", The University of Memphis Publication	<1 %
54	mattermodeling.stackexchange.com Internet Source	<1 %
55	wiredspace.wits.ac.za Internet Source	<1 %

56	"Handbook of Materials Modeling", Springer Science and Business Media LLC, 2005 Publication	<1 %
57	NATO ASI Series, 1984. Publication	<1 %
58	kyusyu.mof.go.jp Internet Source	<1 %
59	www.theses.fr Internet Source	<1 %
60	open.fau.de Internet Source	<1 %
61	Changjian Zhou, Min Zhang, Cary Y. Yang. "Nanocarbon Electronics", Jenny Stanford Publishing, 2020 Publication	<1 %
62	Jiang, Jingwei. "Topology and Electronic Properties of Low-Dimensional Carbon Materials", University of California, Berkeley, 2023 Publication	<1 %
63	Senozan, Selma. "First-Principles Study of GaAs/AlAs Nanowire Heterostructures.", Middle East Technical University (Turkey), 2024 Publication	<1 %
64	etheses.whiterose.ac.uk Internet Source	<1 %
65	gyan.iitg.ernet.in Internet Source	<1 %
66	ir.library.osaka-u.ac.jp Internet Source	<1 %
67	par.nsf.gov Internet Source	<1 %

68	Haihong Huang, Zhengchun Qian, Zhifeng Liu. "Metal Magnetic Memory Technique and Its Applications in Remanufacturing", Springer Science and Business Media LLC, 2021 Publication	<1 %
69	chemistry-europe.onlinelibrary.wiley.com Internet Source	<1 %
70	d-nb.info Internet Source	<1 %
71	dokumen.pub Internet Source	<1 %
72	dos Santos Gomes, José Nuno. "Polaritonics In Nanostructures With 2d Materials And Point Emitters", Universidade do Minho (Portugal), 2024 Publication	<1 %
73	fdocuments.us Internet Source	<1 %
74	www.ee.lut.fi Internet Source	<1 %
75	Abbas Arab, Qiliang Li. "Anisotropic thermoelectric behavior in armchair and zigzag mono- and fewlayer MoS2 in thermoelectric generator applications", Scientific Reports, 2015 Publication	<1 %
76	Fu, Yixing. "Topological Phases of Matter with Disorder and Quasiperiodicity", Rutgers The State University of New Jersey, School of Graduate Studies, 2022 Publication	<1 %
77	Landin, Alyssa Ruth. "The Role of Defects on the Optical, Electronic, and Magnetic	<1 %

	Properties of Iron-sulfur Solids.", University of Colorado at Boulder, 2018 Publication	
78	gcris.iyte.edu.tr Internet Source	<1 %
79	homepages.tuni.fi Internet Source	<1 %
80	opendata.uni-halle.de Internet Source	<1 %
81	worldwidescience.org Internet Source	<1 %
82	"High-performance Sustainable Materials and Structures", Springer Science and Business Media LLC, 2024 Publication	<1 %
83	Price, Conor Jason. "Ab Initio Study of Intercalated TMDCs and Their Superlattices", University of Exeter (United Kingdom), 2024 Publication	<1 %
84	Sak, Berin. "Molecular Dynamics Simulations of GR/GO-Polyurethane/Polyurea Nanocomposites.", Middle East Technical University (Turkey), 2024 Publication	<1 %
85	Sen, Debarati. "Quantum Well Design and Optimization for Enhanced Epsilon-Near-Zero Mode Absorption", State University of New York at Buffalo, 2024 Publication	<1 %
86	Varghese, Seba, Saino Varghese, Sundaram Swaminathan, Krishna Singh, and Vikas Mittal. "Two-Dimensional Materials for Sensing: Graphene and Beyond", Electronics, 2015. Publication	<1 %

87	Yamamoto, Mahito, Sheng Tsung Wang, Meiyan Ni et al. "Strong Enhancement of Raman Scattering from a Bulk-Inactive Vibrational Mode in Few-Layer MoTe2", ACS Nano Publication	<1 %
88	api-depositonce.tu-berlin.de Internet Source	<1 %
89	assets-eu.researchsquare.com Internet Source	<1 %
90	digibuo.uniovi.es Internet Source	<1 %
91	docksci.com Internet Source	<1 %
92	dspace.cuni.cz Internet Source	<1 %
93	ebin.pub Internet Source	<1 %
94	escholarship.org Internet Source	<1 %
95	etd.lib.metu.edu.tr Internet Source	<1 %
96	libjncir.jncasr.ac.in Internet Source	<1 %
97	openscholarship.wustl.edu Internet Source	<1 %
98	www.bremhlr.uni-bremen.de Internet Source	<1 %
99	www.yumpu.com Internet Source	<1 %
100	Ghazwani, Mofareh Ahmed. "A Study of Carbon and Iron Charged Point Defects in	<1 %

	Gallium Nitride: Electronic Structure Implications for High-Power Photoconductive Solid State Switch Applications", University of Missouri - Kansas City, 2022 Publication	
101	Kallem, Aydoğa. "Ab Initio Modelling and Investigation of the Effects of Magnesium Oxide Surface Modifications on Single Atom Catalysis Systems", Middle East Technical University (Turkey), 2024 Publication	<1 %
102	Rafiezadeh, Shohreh. "Electronic, Optical and Catalytic Properties of CoFe2O4from First Principles Including Many-body Effects", Universitaet Duisburg-Essen (Germany) Publication	<1 %
103	Arvydas Tamulis, Mantas Grigalavicius. "The Emergence and Evolution of Life in a “Fatty Acid World” Based on Quantum Mechanics", Origins of Life and Evolution of Biospheres, 2010 Publication	<1 %
104	Electronic Density Functional Theory, 1998. Publication	<1 %
105	Tilak, Nikhil M. "Scanning Tunneling Microscopy Studies of Twisted Van Der Waals Heterostructures", Rutgers The State University of New Jersey, School of Graduate Studies, 2023 Publication	<1 %
106	Ulrich Rössler. "Electrons in a Periodic Potential", Solid State Theory, 2009 Publication	<1 %